NASA/TM—1999-209268

Using High Frequency Focused Water-Coupled Ultrasound for 3–D Surface Depression Profiling

Don J. Roth
Glenn Research Center, Cleveland, Ohio

Mike F. Whalen and J. Lynne Hendricks
Sonix, Inc., Springfield, Virginia

James R. Bodis
Cleveland State University, Cleveland, Ohio

July 1999

The NASA STI Program Office . . . in Profile

Since its founding, NASA has been dedicated to the advancement of aeronautics and space science. The NASA Scientific and Technical Information (STI) Program Office plays a key part in helping NASA maintain this important role.

The NASA STI Program Office is operated by Langley Research Center, the Lead Center for NASA's scientific and technical information. The NASA STI Program Office provides access to the NASA STI Database, the largest collection of aeronautical and space science STI in the world. The Program Office is also NASA's institutional mechanism for disseminating the results of its research and development activities. These results are published by NASA in the NASA STI Report Series, which includes the following report types:

- TECHNICAL PUBLICATION. Reports of completed research or a major significant phase of research that present the results of NASA programs and include extensive data or theoretical analysis. Includes compilations of significant scientific and technical data and information deemed to be of continuing reference value. NASA's counterpart of peer-reviewed formal professional papers but has less stringent limitations on manuscript length and extent of graphic presentations.

- TECHNICAL MEMORANDUM. Scientific and technical findings that are preliminary or of specialized interest, e.g., quick release reports, working papers, and bibliographies that contain minimal annotation. Does not contain extensive analysis.

- CONTRACTOR REPORT. Scientific and technical findings by NASA-sponsored contractors and grantees.

- CONFERENCE PUBLICATION. Collected papers from scientific and technical conferences, symposia, seminars, or other meetings sponsored or cosponsored by NASA.

- SPECIAL PUBLICATION. Scientific, technical, or historical information from NASA programs, projects, and missions, often concerned with subjects having substantial public interest.

- TECHNICAL TRANSLATION. English-language translations of foreign scientific and technical material pertinent to NASA's mission.

Specialized services that complement the STI Program Office's diverse offerings include creating custom thesauri, building customized data bases, organizing and publishing research results . . . even providing videos.

For more information about the NASA STI Program Office, see the following:

- Access the NASA STI Program Home Page at ***http://www.sti.nasa.gov***

- E-mail your question via the Internet to help@sti.nasa.gov

- Fax your question to the NASA Access Help Desk at (301) 621-0134

- Telephone the NASA Access Help Desk at (301) 621-0390

- Write to:
  NASA Access Help Desk
  NASA Center for AeroSpace Information
  7121 Standard Drive
  Hanover, MD 21076

NASA/TM—1999-209268

Using High Frequency Focused Water-Coupled Ultrasound for 3–D Surface Depression Profiling

Don J. Roth
Glenn Research Center, Cleveland, Ohio

Mike F. Whalen and J. Lynne Hendricks
Sonix, Inc., Springfield, Virginia

James R. Bodis
Cleveland State University, Cleveland, Ohio

National Aeronautics and
Space Administration

Glenn Research Center

July 1999

Available from

NASA Center for Aerospace Information
7121 Standard Drive
Hanover, MD 21076
Price Code: A03

National Technical Information Service
5285 Port Royal Road
Springfield, VA 22100
Price Code: A03

Using High Frequency Focused Water-Coupled Ultrasonic Pulses For 3-D Surface Depression Profiling

Don J. Roth
National Aeronautics and Space Administration
Glenn Research Center
Cleveland, OH 44135

and

Mike F. Whalen and J. Lynne Hendricks
Sonix, Inc.
Springfield, VA 22152

and

James R. Bodis
Cleveland State University
Cleveland, OH 44115

Funding for this work came from the NASA HITEMP and COMMTECH programs, and from Sonix, Inc.

ABSTRACT

Surface topography is an important variable in the performance of many industrial components and is normally measured with diamond-tip profilometry over a small area or using optical scattering methods for larger area measurement. A prior study was performed demonstrating that focused *air-coupled* ultrasound at 1 MHz was capable of profiling surfaces with 25 μm depth resolution and 400 μm lateral resolution over a 1.4 mm depth range. In this article, the question of whether higher-frequency focused water-coupled ultrasound can improve on these specifications is addressed. 10 and 25 MHz focused ultrasonic transducers were employed in the water-coupled mode. Time-of-flight images of the sample surface were acquired and converted to depth / surface profile images using the simple relation (d = V*t/2) between distance (d), time-of-flight (t), and the velocity of sound in water (V). Results are compared for the two frequencies used and with those from the 1 MHz air-coupled configuration.

INTRODUCTION

To interface with other solids, many surfaces are engineered via plating, coating, machining methods, etc. to produce a functional surface ensuring successful end products. Additionally, *subsurface* properties such as hardness, residual stress, deformation, chemical

composition, and microstructure are often linked to surface characteristics. Surface topography, therefore, contains signatures of the surface and possibly links to volumetric properties, and as a result serves as a vital link between surface design, manufacturing, and performance (refs. 1,2). Hence, surface topography can be used to diagnose, monitor and control fabrication methods. Ref. 1 states that "it is becoming increasingly obvious that a full understanding of the link between surface topography and functional performance can only be realized if a 3-D (areal) approach to surface characterization is used."

Diamond-tipped profilometry is the usual method for obtaining 2-D (line) precision surface depression variation in material samples and can resolve variation to 0.001 μm or better (ref. 1). However, this method requires contact with the sample which can cause undesirable alterations to the sample surface if further characterization is required. Additionally, the method is very slow and impractical for obtaining detailed, large scan area profiles, and has limited (μm-scale) vertical depth range. Optical scattering provides a large area profiling capability but requires lasers, sometimes an array of detectors, a light-reflective surface, and also provides only limited (μm-scale) vertical depth range (ref. 3). Scanning probe microscopy can provide noncontact surface profiling methods but is applicable only up to the hundreds of microns level and is not practical for macro-topography or large area profiling (ref.1). Ultrasonic methods have shown potential for surface profiling in the micron resolution regime in both the amplitude (scattering) and time-of-flight (which provides a direct measurement of depth) mode as shown by ref. 4. Ref. 4 reported surface profiling results with depth resolution in the 1 to 40 μm range using *water-coupled* ultrasonics in both peak amplitude and time-of-flight mode employing frequencies up to 30 MHz. In that study, line plots of ultrasonic peak amplitude and time-of-flight versus surface condition (roughness and sinusoidal height, respectively) were presented for plate and cylindrical samples. Ref. 5 performed an in-depth study of air-coupled ultrasonic surface profiling using a commercialized ultrasonic profilometry scan system to profile surfaces in three-dimensions (3-D) and showed that 1 MHz air-coupled ultrasound was capable of profiling surfaces with 25 μm depth resolution and 400 μm lateral resolution over a 1.4 mm depth range.

In this study, the authors build on the investigations of refs. 4 and 5, focusing on the effectiveness of the water-coupled ultrasonic profiling method in the pulse-echo time-of-flight mode for generating accurate 3-D surface profiles. The water-coupled ultrasonic method is worth investigating further because, as compared to the air-coupled method, it theoretically results in greater depth range over which optimal depth resolution can be obtained as well as greater spatial resolution (This will be discussed in the BASIC PRINCIPLES section). Furthermore, in practice, greater depth resolution may be possible with water-coupled ultrasonics as compared to air-coupling. The water-coupled ultrasonic method also offers the advantage of being useable in a wet environment (where air coupling is not possible) such as that encountered on turning and milling centers, and also where the stylus contact method or laser impingement is undesirable (ref. 4). In this study, nominal frequencies of 10 MHz and 25 MHz are employed. Results are shown for several proof-of-concept samples (a Kennedy half-dollar, and wedge-shaped ceramic sample), and for plastic samples burned in microgravity on the STS-54 space shuttle mission. Comparison between water-coupled and air-coupled results are presented.

BASIC PRINCIPLES

Obtaining Surface Profiles from Time-of-Flight Information

The ultrasonic profiling method uses an ultrasonic focused beam as a stylus with the beam impinging on the sample surface at nominally-perpendicular incidence as shown in figure 1. Time-of-flight images using a 13-bit data gate are used to allow fine time resolution over significant surface depressions (ref. 5). Surface depression profiles are calculated based on the time-of-flight images. The method relies mainly on knowledge of the velocity of ultrasound through water which remains reasonably constant at all times and locations if temperature is held constant (as in a large ultrasonic tank in a temperature-regulated room). The method as implemented on the Sonix, Inc. Flexscan ultrasonic c-scan system (ref. 6) using the Sonix STR*81GU analog-to-digital converter board, has potential for extremely high speed. The sample should be placed on a support of uniform flatness and parallelness but provisions in the commercial software allow releveling of the initial surface profile as is common in most commercially-available diamond-tip profilometers.

In figure 1, $d_{x,y}$ is the distance at any x,y location between the sample and the ultrasonic transducer and is variable due to the surface irregularity. If the ultrasonic system is activated and an x,y ultrasonic scan is performed over the sample, ultrasonic reflections off of the top sample surface will be obtained. Normalized surface depression at any x,y location ($Z_{x,y}$) is determined from:

$$Z_{x,y} = \frac{V_{water}}{2}(t_{x,y} - t_{\min}) \tag{1}$$

where $t_{x,y}$ is the time-of-flight of the first front surface reflection at any x,y surface location (and will vary with $Z_{x,y}$ and $d_{x,y}$), t_{min} is the time-of-flight corresponding to the highest surface position on the sample front surface, and V_{water} is the velocity of ultrasound in water (dependent upon the temperature and is ~ 1.48 cm/μsec at 68ºF [ref. 7]).

Time and Distance Resolution Determination

Time resolution (TR) of the ultrasonic data acquisition for the commercial scan system employed in this investigation can be defined in terms of analog-to-digital (a/d) sampling rate (SR) according to:

$$TR(\eta\,\mathrm{sec}) = \left(\frac{1}{SR[GHz]}\right) \tag{2}$$

for 13-bit data gate length (GL) ≤ 8192 points (ref. 5).

Distance / depth resolution (DR) for surface profiling is obtained to a first approximation from:

$$DR(\mu m) = \frac{V_{water}(mm/\mu\sec) \bullet TR(\eta\sec)}{2} \tag{3}$$

For water at 68ºF (V_{water} = 1.48 mm/μsec) (figure 2, ref. 7), this time resolution translates into DR to a first approximation of ~ 0.74 μm from eq. (3). The error in this value can be found by performing the traditional error analysis where (ref. 8):

$$\sigma_{DR} = \sqrt{\left(\frac{\partial(DR)}{\partial V_{water}}\right)^2 \sigma_{Vwater}^{\ 2} + \left(\frac{\partial(DR)}{\partial(TR)}\right)^2 \sigma_{TR}^{\ 2}} \tag{4}$$

The error in time resolution (TR) can be expressed in terms of the analog-to-digital sampling rate (SR) according to:

$$\sigma_{TR}(\eta\sec) = \frac{1}{2 \bullet SR(GHz)} \tag{5}$$

so that for 1 GHz a/d sampling rate σ_{TR} = 0.5 ηsec. Using σ_{Vwater} = 0.005 mm/μsec as the error in measuring water velocity, a $\sigma_{DR} \cong$ 0.37 μm is obtained from eq. (4). Adding this error to the result of eq. (3) gives a best case (ideal conditions) estimate for vertical distance resolution (DR) of approximately 1.1 μm for 1 GHz sampling rate using water coupling.

Vertical Depth Range

With a 13-bit acquisition limit, the improvement in vertical depth range over which time/ depth resolution stays constant is 32-fold as compared to a 8-bit acquisition limit. Specifically, for 1 GHz sampling rate (1 data point = 1 ηsec), water at 68ºF (V_{water} = 1.48 mm/μsec), and vertical depth range = velocity*(maximum gate length in time [8192 ηsec])/2 in the pulse-echo configuration, a 6.06 mm vertical depth range is obtained with 8192 (13-bit) data point acquisition limit versus a 0.19 mm vertical depth range obtained with a 256 (8-bit) data point acquisition limit. Furthermore, the 6.06 mm vertical depth range is 4.35x greater than that obtained using air-coupled ultrasonics (where 1.393 mm vertical depth range was obtained) (ref. 5).

Transducer Focal Spot Size

Transducer focal spot diameter determines the area of the specimen surface sampled. It is likely to limit sample feature resolution, although complex scattering interactions of ultrasound off surface features closely spaced together may result in “improved” or worsened resolution. It is expected that the focal spot diameter would limit the lateral resolution capability. A relationship exists between focal spot diameter of an ultrasonic

beam (ϕ) at 50% drop in sound pressure (- 6dB point), ultrasonic wavelength (λ), transducer focal length (L_f), and transducer element diameter (X) according to (ref. 7):

$$\varphi = 2.44 \bullet \lambda \bullet \frac{L_f}{X} \tag{6}$$

Ultrasonic wavelength (λ) can be expressed in terms of transducer frequency and ultrasonic velocity in water (V_{water}) according to:

$$\lambda = \frac{V_{water}}{f} \tag{7}$$

Noting that V_{water} = 1.48 mm/μsec at 68ºF and substituting eq. (7) into eq. (6) gives:

$$\varphi(\mu m) = 2440 \bullet \frac{1.48(mm/\mu \sec)}{f(MHz)} \bullet \frac{L_f(mm)}{X(mm)} \tag{8}$$

Figures 3 and 4 show the relationship between focal spot size, transducer frequency, focal length, and element diameter. For example, from eq. (8) it has been found that using a 25 MHz center frequency focused transducer with a focal length of 38.1 mm and 6.35 mm element diameter results in a focal spot diameter of ~ 900 μm. Using a 10 MHz center frequency focused transducer with a focal length of 25.4 mm and 12.7 mm element diamater results in a focal spot of ~ 700 μm. These values are significantly larger than that for typical diamond tip profilometers that have stylus diameters on the order of 4 μm. Laser systems achieve spot sizes on the order of 25 μm as well (ref. 3).

Echo Features used for Time-of-Flight

It is recommended that the precise time-of-flight of the front surface echoes is measured either to the intersection of a gate and the leading edge of the echo (the height level of the gate being set by the user), or by gating a selected peak of the echo (again determined by the user). Gating the leading edge has generally produced better results than gating the peak and is recommended. Such gating is illustrated in figure 5.

EXPERIMENTAL PROCEDURE

Materials

First, to benchmark the depth resolution and quantitative accuracy of the ultrasonic profiling system at 10 and 25 MHz, an aluminum step wedge was fabricated having steps successively separated in depth by 3, 6, 9, and 12 μm, respectively (or in terms of distance from the wedge top surface, 3, 9, 18, and 30 μm, respectively.) The machining deviation for the steps was ± 1 - 2 μm. Secondly, to benchmark the lateral resolution capability of the

ultrasonic profiling system at 10 and 25 MHz, an aluminum block was manufactured with a series of channels separated by increasing distance. The channels were separated by 0, 37, 96, 101, 113, 120, 130, 157, 177, 236, 283, 381, 484 and 577 μm. The machining deviation for the channel separation was ± 10 μm. Then, several proof of concept samples were profiled which included a ceramic wedge sample having a smooth ~ 300 μm thickness gradient from left-to-right edge, and a Kennedy half-dollar coin (figure 6). The next samples profiled were "real world" samples that required knowledge of surface depression information. They were ~ 0.6 cm by ~ 3 cm plastic samples that were the objects in a microgravity combustion space experiment onboard the space shuttle (mission STS-54). It was desired to obtain whole area surface depression profiles to characterize the microgravity burning of these samples. Figure 7 shows several diamond tip profilometry line scans across the surface of one of the burned plastic samples. The burn was started at the right end of the sample. The burn caused 1) a loss of material from the 23 to the 15 mm locations and 2) a lip to form at the ~ 15 mm mark that was ~ 0.2 mm higher than the starting surface height. A maximum depth of 0.895 mm was obtained by the diamond-tip profilometry.

Ultrasonic Profiling

Ultrasonic time-of-flight c-scans were performed on all samples with a Sonix ultrasonic scan system with a screw-driven motorized bridge assembly that has a software interface for on-line surface profilometry (ref. 5). A Panametrics, Inc. 10 MHz nominal center frequency broadband transducer of focal length = 25. 4 mm (1.0 in.) and element diameter = 12.7 mm (0.5 in.) and Harisonic (-S type) 25 MHz nominal center frequency broadband transducer of focal length = 38.1 mm (1.5 in.) and element diameter = 6.35 mm (0.25 in.) were employed. Actual center frequencies (as obtained from the magnitude plots of the discrete fourier transforms) for a pulse reflected from the front surface of an aluminum plate placed at the focal distance were 23 - 24 MHz for the 25 MHz transducer and 9 MHz for the 10 MHz transducer. 1 GHz a/d sampling rate and 13-bit (8192 bits) time-of-flight data gates were employed. Scan (length) and step (width) increments used for the samples were 95 μm in hopes of obtaining finer averaged lateral detail as was done in prior ultrasonic studies (ref. 4.). Scans were on the order of 400 scan points by 400 scan lines. Using the Sonix STR*81GU analog-to-digital (A/D) converter board, linear scan speeds were on the order of 5 mm/sec - 30 mm/sec at the 95 μm scan / step increment with 4 - 32 waveform averages performed in software as the scan progressed. (Waveform averaging "on-the-fly" using the sum of successive waveform acquisitions was used to obtain higher signal-to-noise ratios at the expense of scan speed.) A UTEX 340 pulser-receiver (200 MHz bandwidth) was used to pulse the transducer and receive the ultrasonic signal, and to trigger the A/D board. Baseline instrumentation set-up is shown in figure 8.

During initial set-up, the transducer was focused at the sample front surface (in a mid-region of the sample) by adjusting its distance from the sample and by adjusting its gimbal angle to obtain the time location where the highest amplitude for the front-surface–reflected echo occurred on the digital oscilloscope. (The variations in focal length caused by surface depressions in the sample did not appear to significantly affect results.) A single data gate was used intersecting the negative leading edge of the front surface-reflected echo (rf waveform display) which was heavily driven into saturation (over 100% full scale height of

the oscilloscope display) similar to what is shown in figure 5. Gate length was set to cover the entire time extent corresponding to the surface variation being tracked. Water temperature was 66ºF ± 0.1ºF.

Using eq. (1), surface depression profiles were calculated from raw time-of-flight images obtained from the leading edge-gated front surface echo (ref. 5). Sample profile images were leveled as needed by subtracting from the sample time-of-flight scan an identical scan of the support plate (figure 1) on which the sample sat. Profile results are presented in both 2-D and 3-D image displays as obtained directly from the Sonix system, and were low-pass filtered in some cases for noise minimization. (In typical profilometry systems, low-pass filtering historically has been used to eliminate the longer wavelength (form and waviness) components (refs. 1,2)). Appropriate 8-bit (256 levels) color schemes are chosen to highlight the results. Removal of extreme high and low values caused by randomly improper gating was performed where necessary using an option in the surface profilometry system. At these locations, nearest neighbors averaging was implemented to replace the value. In general, eight nearest valid neighbors are used in the calculation of the average. Exportation of the data for off-line processing is an option in the software so that one can use his or her preferred image processing and display package.

RESULTS & DISCUSSION

Channeled Aluminum Block

The ultrasonic time-of-flight images for the channeled aluminum block are shown in figure 9 at 25 MHz and 10 MHz. Channel separation as small as ~ 180 μm was resolvable at 25 MHz (~ $1/5^{th}$ the nominally-predicted focal spot size) and as small as 250 – 300 μm at 10 MHz (~ 1/2 - $1/3^{rd}$ the nominally-predicted focal spot size).

Stepped Aluminum Block

Figures 10 and 11 shows 2-D and 3-D views of ultrasonic surface profiles of the stepped aluminum block at 25 MHz and 10 MHz, respectively. The ultrasonic method was able to discriminate surface depressions separated by as small as 3 μm (which was the smallest depression used in this investigation) at 25 MHz, and separated by as small as 6 μm at 10 MHz. Although the individual depression regions are clearly delineated as shown by the color differences of the regions, oscillating background noise is superimposed on the line profile and image. The majority of this noise appears to be from vibration caused during the scan by the motor / bridge assembly movement (see FURTHER DISCUSSION section below). This noise was ~ 5 - 15 μm peak-to-peak and fairly regularly- and finely-spaced. This led the authors to apply a low-pass filter to the surface depression profile which resulted in a smoothing effect as shown in figure 10b. Figure 10c shows a three-dimensional representation of the ultrasonically-derived surface depression map. Figure 10d shows a line profile for one typical scan line from the low-pass filtered image of figure 10b. Figure 10e shows a line profile for one typical scan line from the low-pass filtered image of figure 10b. The latter figure shows the smoothing effect of the low-pass filter operation. The

oscillations are still present but to a significantly lesser extent. More sophisticated filtering processes might allow further reductions in the noise.

Table I compares the mean (± deviation) values from the low-pass filtered ultrasonically-derived surface depression map with that obtained from the diamond-tip profilometry. The mean (± deviation) values were obtained by drawing a best fit horizontal line through the oscillating line profile (figure 10e) of each individual step section. In this manner, an equal "amount" of deviation was placed above and below the line. (Using the line profile from the same location from the non-filtered image results in about the same mean values but higher deviations due to the unfiltered noise.) Reasonable agreement is observed between diamond-tip and ultrasonic values for surface depression.

Table I. Comparison of surface depression magnitude from ultrasonic scan and diamond-tip profile measurements in the stepped Aluminum block for 25 MHz results.

Step	Cumulative Surface depression from diamond-tip profile (μm)	Mean (± deviation) Surface depression from ultrasonic scan (μm)
A	3	4 ± 4
B	9	8 ± 3
C	18	15 ± 3
D	30	23 ± 3

Any differences in surface topology values between the ultrasonically-derived values and the diamond-tip profile measured values are likely due to1) the use of a slightly incorrect value for water velocity (V_{water}) and 2) the errors resulting from the leading edge of the front surface echo pulse not being fully vertical in nature (possibly causing quantization errors) or identical in morphology at every scan position, the background noise inherent in the scan system.

Ceramic Wedge Sample

Figure 12 shows 2-D and 3-D views of the ultrasonic surface profile of the ceramic wedge at 25 MHz and a line profile for one scan line. Maximum surface depression magnitude is ~ 300 which is about the same as that measured from micrometers. Profiles at 10 MHz were nearly identical.

Kennedy Half-dollar

Figures 13 and 14 show ultrasonic surface profiles for the Kennedy half-dollar at 25 MHz and 10 MHz. Consider figure 13 which shows results at 25 MHz. The black areas indicate areas where significant ultrasonic scatter prevented ultrasound from reflecting back to the transducer. Upon extreme value filtering (with replacement by average of nearest neighbors) of these pixels (figure 13b), a quite accurate representation of the coin is obtained. The 3-D

view of the filtered profile clearly shows the topographical features of the coin. Measurements off of the ultrasonic surface profile for the coin revealed a surface depression maximum ~ 200 – 250 μm which agreed well with touch probe maximum depression measurements (similar to micrometer) of ~ 250 μm. As shown in figure 14d, use of 10 MHz reduced the scatter (less black areas) but also reduced the definition as compared to 25 MHz. This is consistent with the fact that the observed lateral resolution was better at 25 MHz than at 10 MHz. Defocusing the 25 MHz transducer (moving closer to the coin by 5 and 10 μsecs in two separate trials) also resulted in a moderate reduction in the scatter at the significant expense of definition (figures14b and c).

Burned Space Experiment Samples

Figures 15 and 16 show the ultrasonic surface profiles at 25 MHz and 10 MHz, respectively, for the burned space experiment samples. Consider figure 15 which shows results at 25 MHz. The black areas indicate areas where significant ultrasonic scatter prevented ultrasound from reflecting back to the transducer. Upon extreme value filtering (with replacement by average of nearest neighbors) of these pixels (figure 15b), credible morphological representations of the burn profiles were obtained. However, due to the significant scatter and resulting filtering process, the maximum depth recorded from the ultrasonic profile was on the order of 500 μm as compared to 895 μm recorded from diamond-tip profilometry. As expected, the results at 10 MHz resulted in less scatter than at 25 MHz, and the maximum depth recorded at 10 MHz was on the order of 700 μm which more closely agreed with results from diamond-tip profilometry.

WATER- VS. AIR-COUPLED COMPARISONS

In comparing the surface profiles of the Kennedy half-dollar (extreme-value filtered) obtained with 25 MHz water-coupling and 1 MHz air-coupling (figure 17), the greater depth and lateral resolution of the water-coupled method is clearly illustrated. The water-coupled profiles provide much greater definition than do the air-coupled profiles. The results seen in this investigation of water-coupled ultrasonic profilometry at 25 MHz, as compared to air-coupled ultrasonic surface profilometry at 1 MHz (ref. 5), represent:

- an 8x improvement in depth resolution (3 μm vs. 25 μm seen in practice) (mainly due to minimal turbulence in the water-coupled situation as compared to the air-coupled situation)
- at least a 2x improvement in lateral resolution (180 μm vs. 400 μm calculated and observed in practice) (due to the fact that 25 MHz water-coupling represents a 25x increase in frequency over 1 MHz air-coupling, which offsets the air-coupled advantage of 1/5x reduced ultrasonic velocity in air as compared to that in water [see eq. (8)])
- a 4x improvement in vertical depth range (calculated [see discussion on *Vertical Depth Range*]).

However, significantly more scatter will be present in the non-extreme value filtered images of the higher-frequency water-coupling configuration, and likely result in less accurate overall quantitative depth profiling.

FURTHER THOUGHTS

The most significant factor affecting practical utilization of the water-coupled ultrasonic method of surface profiling as described in this study is the scattering effect when high-frequency ultrasound encounters non-perpendicular surfaces and does not reflect back to the transducer. It was shown that in some cases (such as for the Kennedy half-dollar), extreme value filtering / nearest neighbors replacement algorithms can be successfully employed to obtain an accurate surface profile even in the presence of major scatter. For other samples, this strategy might not be as successful (such as for samples having sharp surface gradients and relatively rough surfaces as was seen for the burned plastic samples).

Additionally, the analysis of distance / depth resolution given in the BASIC PRINCIPLES section does not take into account error due to electromagnetic interference that superimposes itself upon the signal, scattering effects that result in the front surface echo being intersected by the time gate in an inconsistent manner, a time-related "jitter" (oscillation) that was observed in the signal possibly due to vibration (external and that due to motor / bridge assembly movement) and water currents (from temperature and pressure variations), and other ultrasonic system-related effects. It is these factors that likely cause the most severe error in this method, with vibration from the motor / bridge assembly movement being the most significant factor. Vibration isolation methods need to be employed to minimize the effects of vibration, and smoother bridge translation mechanisms need to be utilized.

Potentially, using different pulsing mechanisms and changes in transducer design can result in more highly-vertical leading edges thus minimizing the error caused by the front surface echo being intersected by the time gate in an inconsistent manner. Temperature effects on ultrasonic velocity in water were found to be small; a temperature variation from 68ºF to 69ºF was calculated to cause less than 0.1% velocity variation (figure 2). Error due to electromagnetic interference can be minimized with signal averaging.

This method is easily applicable to cyclindrical samples and other curved shapes as was demonstrated in the water-coupling study of ref. 4 and air-coupling study of ref. 5.

CONCLUSIONS

Using a commercialized ultrasonic profilometry system, time-of-flight images of sample surfaces were acquired with 10 and 25 MHz water-coupled ultrasound and converted to depth / surface profile images using the simple relation ($d = V*t/2$) between distance (d), time-of-flight (t), and the velocity of sound in water (V). The surface profile results seen in this investigation for 25 MHz water-coupled ultrasound, as compared to those for 1 MHz air-coupled ultrasound, represent an 8x improvement in depth resolution (3 μm vs. 25 μm seen in practice), at least a 2x improvement in lateral resolution (180 μm vs. 400 μm calculated and observed in practice), and a 4x improvement in vertical depth range (calculated). In most cases, impressive topographical representations were obtained for all samples when compared with diamond-tip profiles and measurements from micrometers.

The method is completely nondestructive and requires only water as a coupling fluid, and can profile large areas only limited by the scan limits of the particular ultrasonic system. The most significant factor affecting practical utilization of the water-coupled ultrasonic method of surface profiling as described in this study is the scattering effect when high-frequency ultrasound encounters non-perpendicular surfaces and does not reflect back to the transducer. It was shown that in some cases (such as for the Kennedy half-dollar), extreme value filtering / nearest neighbors replacement algorithms can be successfully employed to obtain an accurate topological representation even in the presence of major scatter. Overall quantitative agreement, however, remains difficult in the presence of significant scatter.

REFERENCES

1. Stout, K.J., Sullivan, P.J., Dong, W.P., Mainsah, E., and Luo, N., Chapters 1 and 2, **The Development of Methods For The Characterisation of Roughness in Three Dimensions,** Publication no. EUR 15178 EN of the Commission of the European Communities.
2. **Surface Texture (Surface Roughness, Waviness, and Lay)**, ASME B46.1-1995.
3. Harding, K.G., Laser Scatter Surface Finish Measurement Techniques, **Laser Institute of America Proceedings of the Optical Sensing and Measurement Symposium – ICALEO'91,** Nov 3-8, 1991, Vol. 73, 1992.
4. Blessing, G.V. and Eitzen,D.G., Ultrasonic Sensor for measuring surface roughness, **SPIE Vol. 1009 Surface Measurement and Characterization** (1988).
5. Roth, D.J., Kautz, H.E., Abel, P.B., Whalen, M.F., Hendricks, J.L., and Bodis, J.R., 3-D Surface Depression Profiling Using High Frequency Focused Air-Coupled Ultrasonic Pulses, NASA TM-1999-209053, 1999.
6. FlexSCAN-C Ultrasonic C-Scan User's Guide, Version 4, January 1998, Sonix, Inc., 8700 Morrissette Drive, Springfield, VA 22152.
7. **Nondestructive Testing Handbook**, second edition, Volume 7 Ultrasonic Testing, eds. Birks, A.S., Green, R.E., and Mcintire, P. American Society For Nondestructive Testing, 1991, p. 225, 833.
8. Bevington, R.P., **Data Reduction and Uncertainty Analysis for the Physical Sciences**, Chapter 4, 1969. McGraw-Hill, New York, NY.
9. Roth, D.J., Kiser, J.D., Swickard, S.M., Szatmary, S.M. and Kerwin, D.P., Quantitative Mapping of Pore Fraction Variations in Silicon Nitride Using an Ultrasonic Contact Scan Technique, **Res. Nondestr. Eval**., Vol. 6, 1995, pp. 125-168.

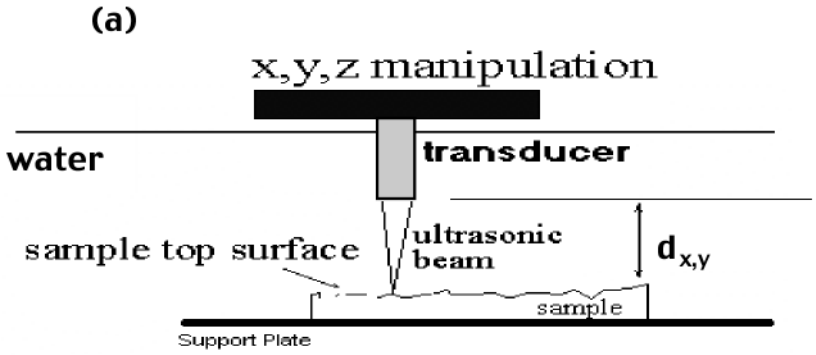

Figure 1.—Experimental set-up for ultrasonic surface profilometry (a) schematic of basic principle and set-up for samples.

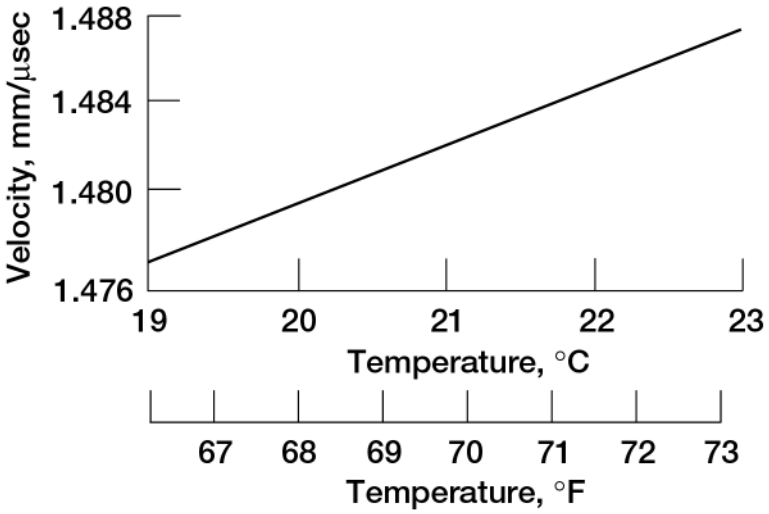

Figure 2.—Ultrasonic velocity of water versus temperature from ref. 1. $C = (1410 + 4.21T - 0.037T^2) \times 10^{-3}$ where C = water velocity (mm/μsec) and T= water temperature (°C).

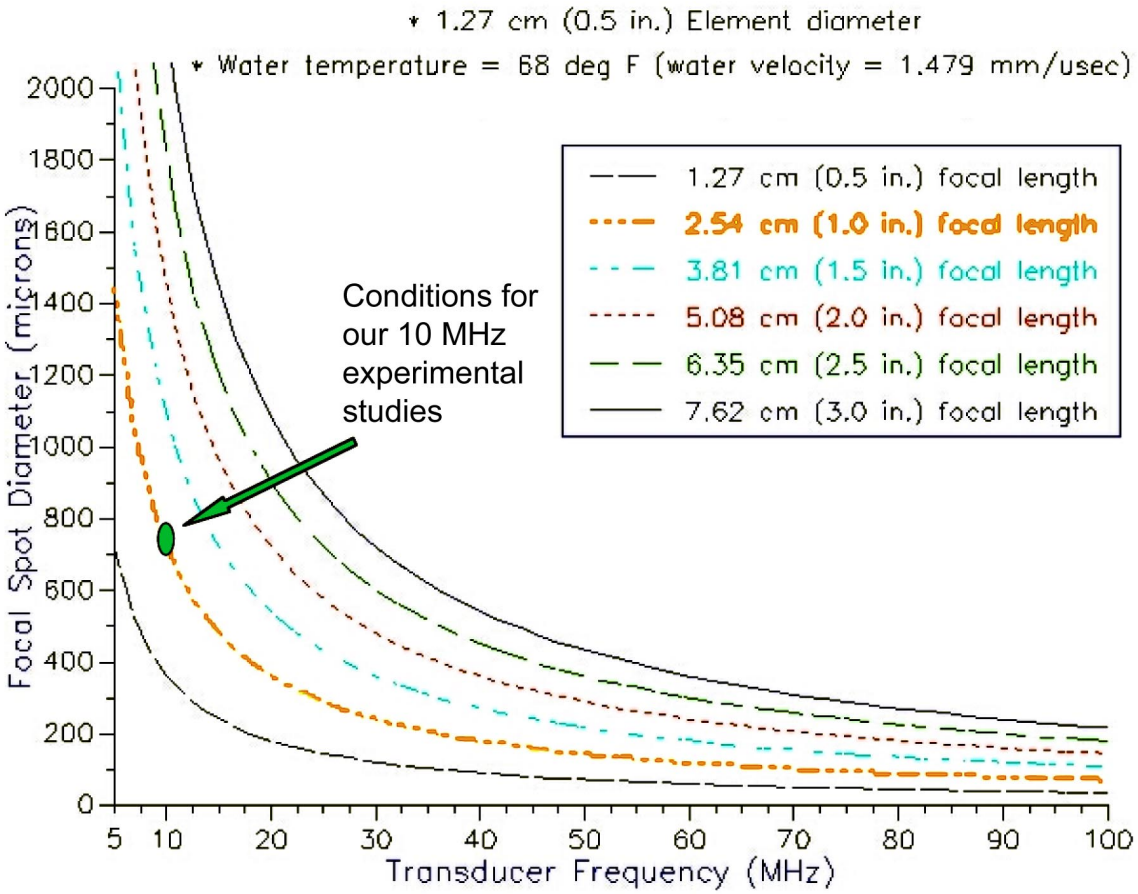

Figure 3.—Predicted Relationship from Eq. (B3) between focal spot size, transducer frequency, focal length, and element diameter for 1.27 cm element diameter.

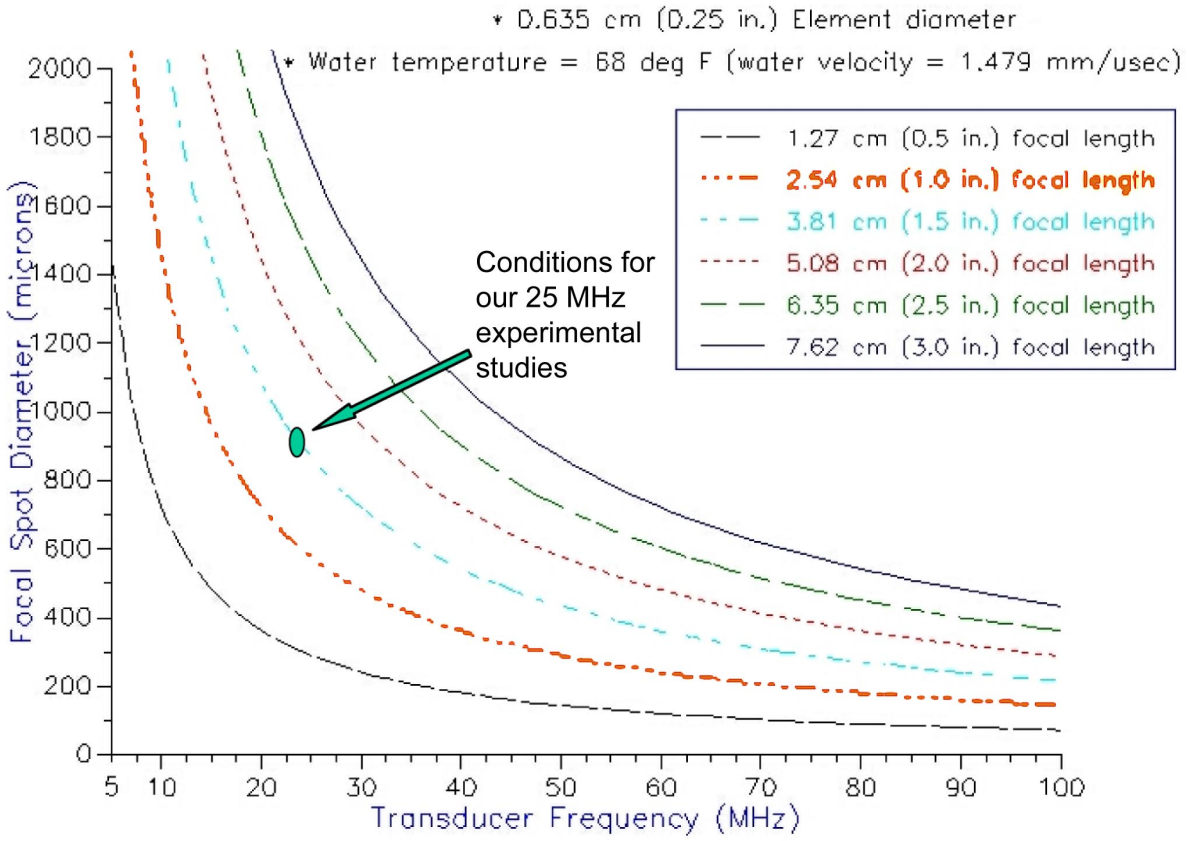

Figure 4.—Predicted Relationship from Eq. (B3) between focal spot size, transducer frequency, focal length, and element diameter for 0.635 cm element diameter.

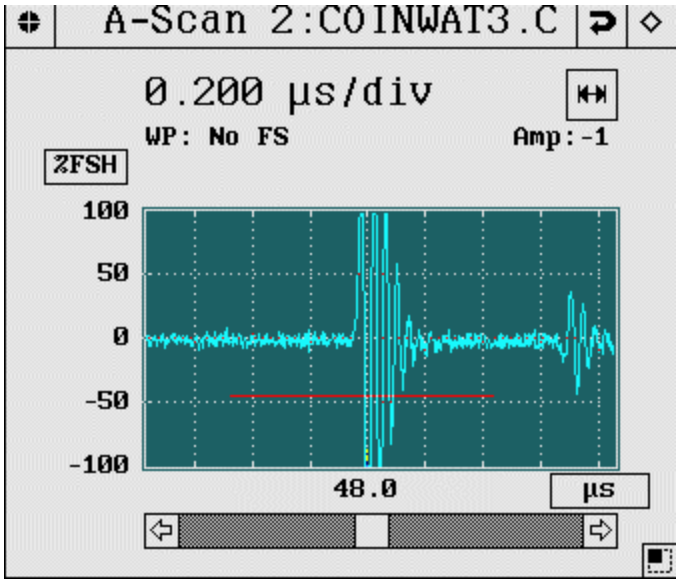

Figure 5. Time gating for ultrasonic surface profilometry using gate intersecting leading edge of front surface echo.

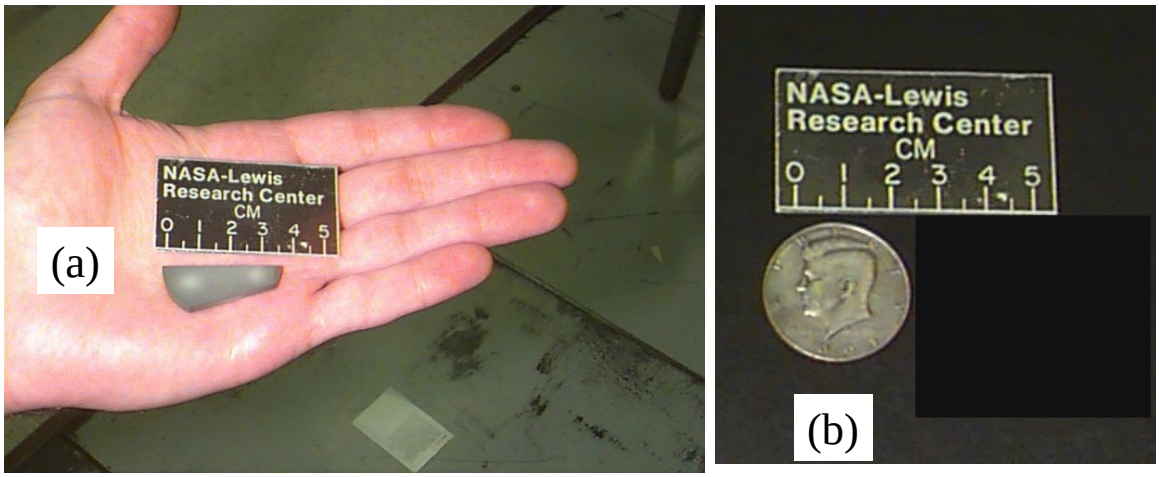

Figure 6. Photos of proof-of-concept samples (a) ceramic wedge (b) Kennedy half-dollar coin.

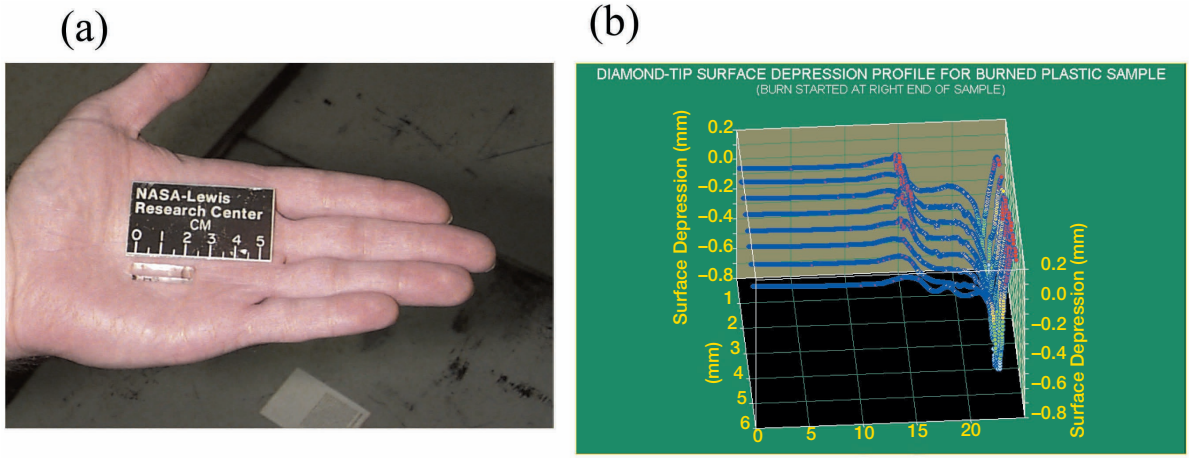

Figure 7. Plastic sample that was the object in a microgravity combustion space experiment onboard the space shuttle (mission STS-54) (a) photograph (b) diamond tip profile.

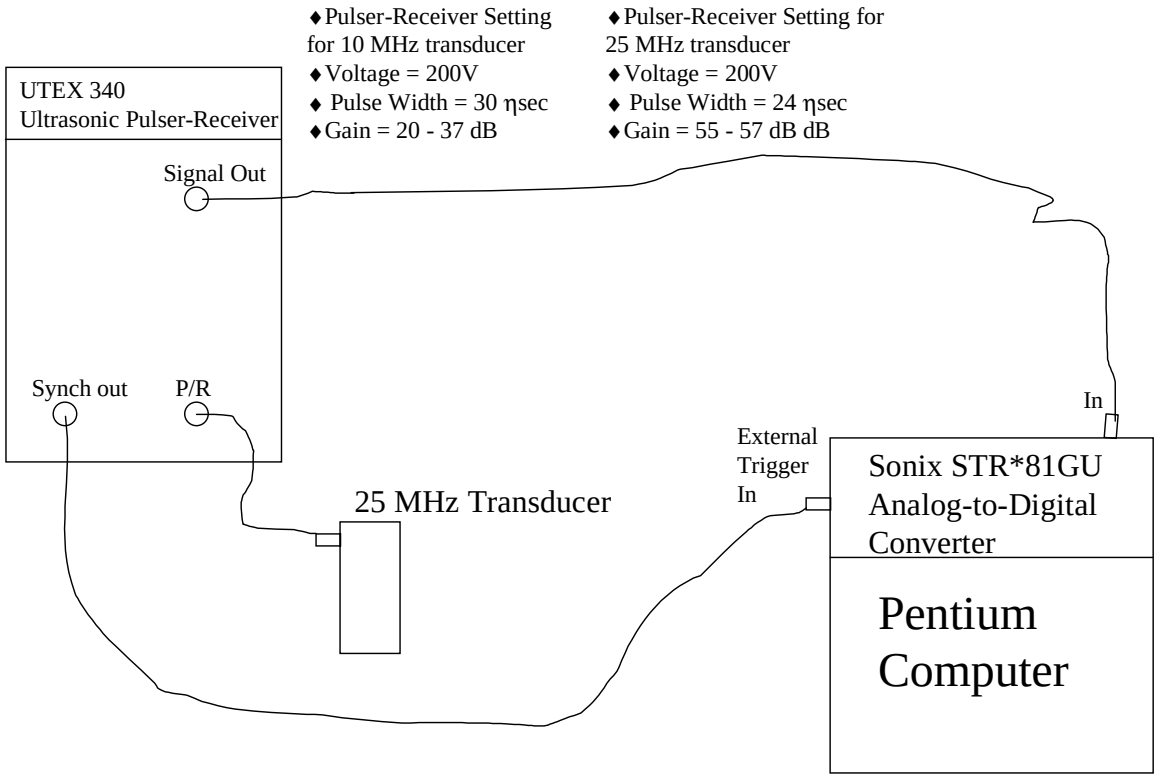

Figure 8. Instrumentation set-up.

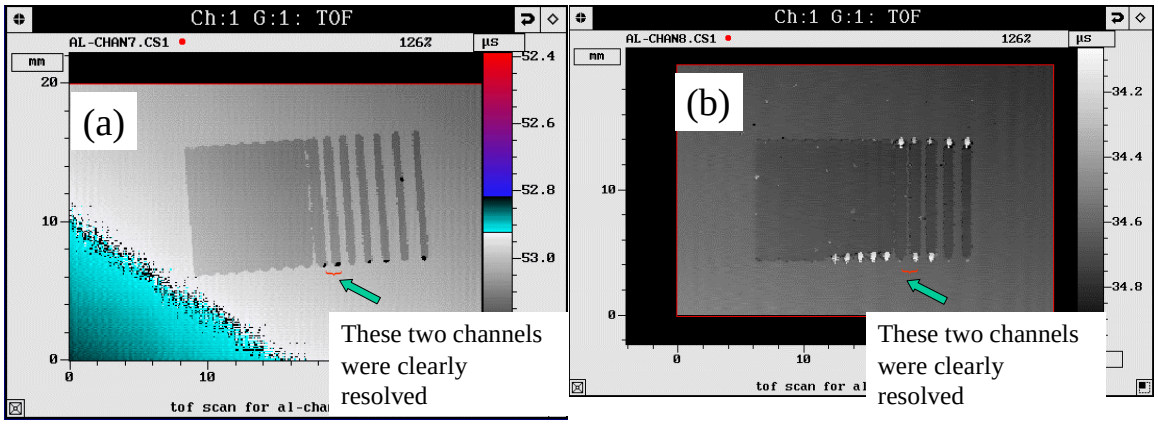

Figure 9. Time-of-flight to Front Surface Profile of Channeled Aluminum Block for Determination of Lateral Resolution Capability of Water-coupled Ultrasonic Surface Profilometry at (a) 25 MHz and (b) 10 MHz. Shows the lateral / spatial resolution available is ~ 180 µm at 25 MHz and ~ 250 - 300 µm at 10 MHz.

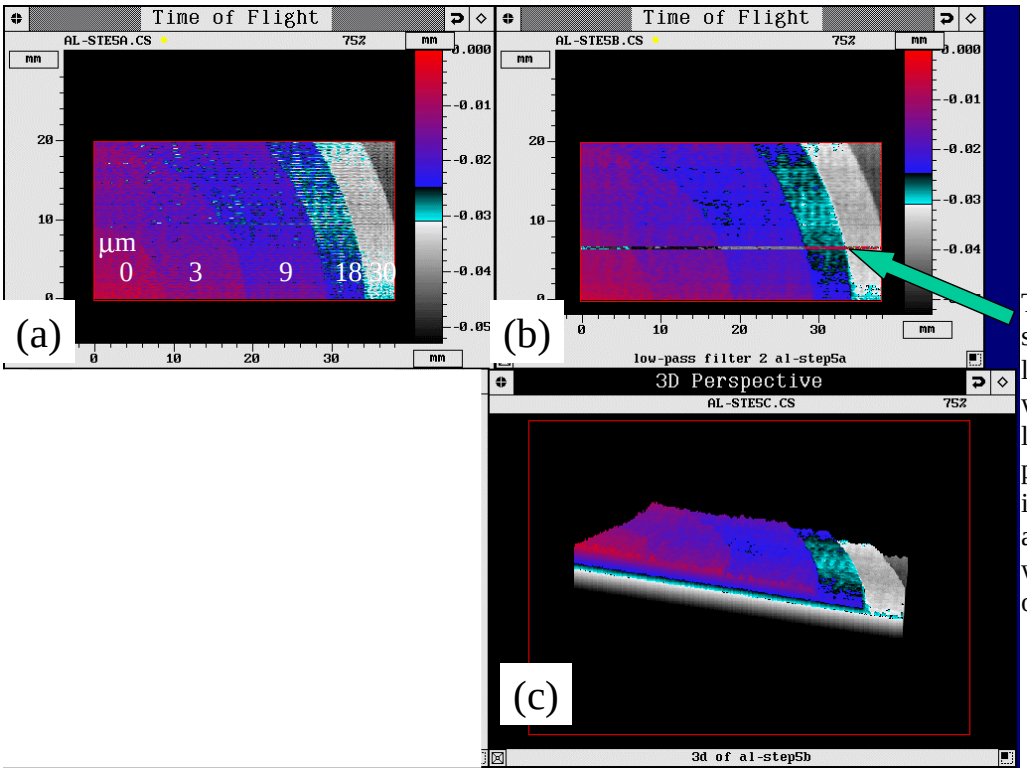

Figure 10. Surface Profile of Aluminum Step Wedge for Determination of Depth Resolution Capability of Water-coupled Ultrasonic Surface Profilometry at 25 MHz. (a) As-obtained time-of-flight profile of aluminum step wedge showing the depth resolution available with the experimental set-up of this study is ~ 3 µm. Numbers above image indicate step depth from top (0) in µm. (b) after low-pass filtering (smoothing). (c) Three-dimensional view of (b).

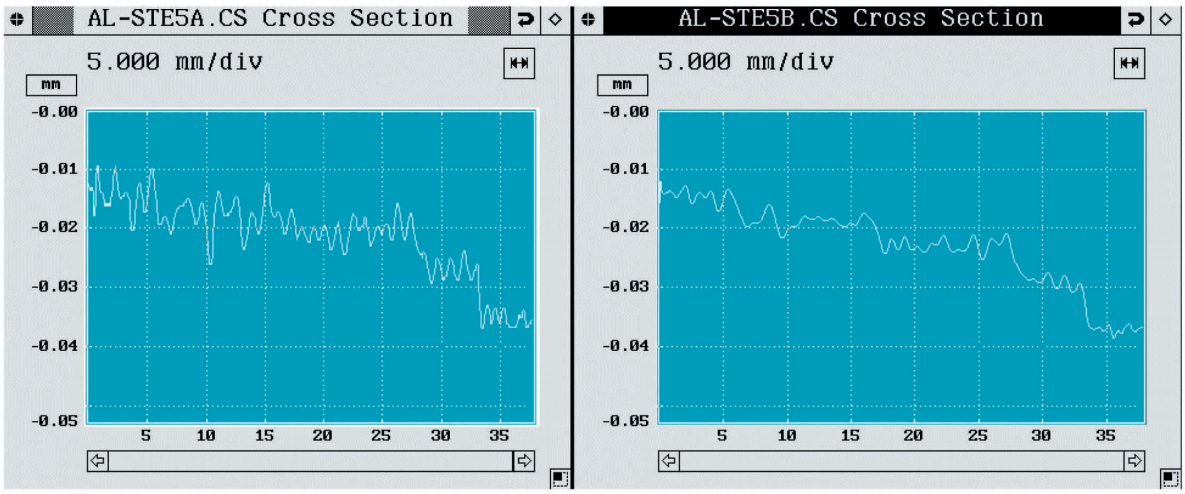

Figure 10 (cont). (d) line profile through surface profile in (a) as indicated on (b). (e) line profile through surface profile in (b) at same location showing the effect of low-pass filtering.

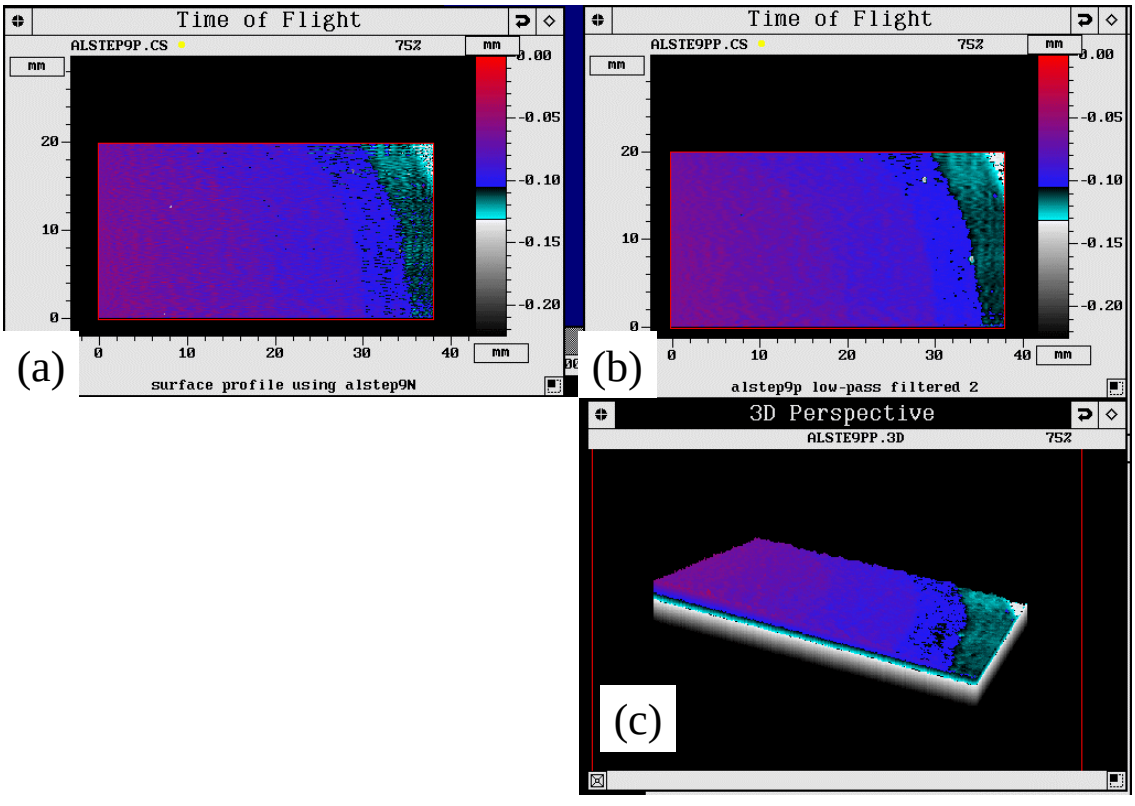

Figure 11. Surface Profile of Aluminum Step Wedge for Determination of Depth Resolution Capability of Ultrasonic Surface Profilometry at 10 MHz. (a) As-obtained time-of-flight profile of aluminum step wedge showing the depth resolution available is ~ 6 μm. Numbers above image indicate step depth from top (0) in μm. (b) after low-pass filtering (smoothing). (c) Three-dimensional view of (b).

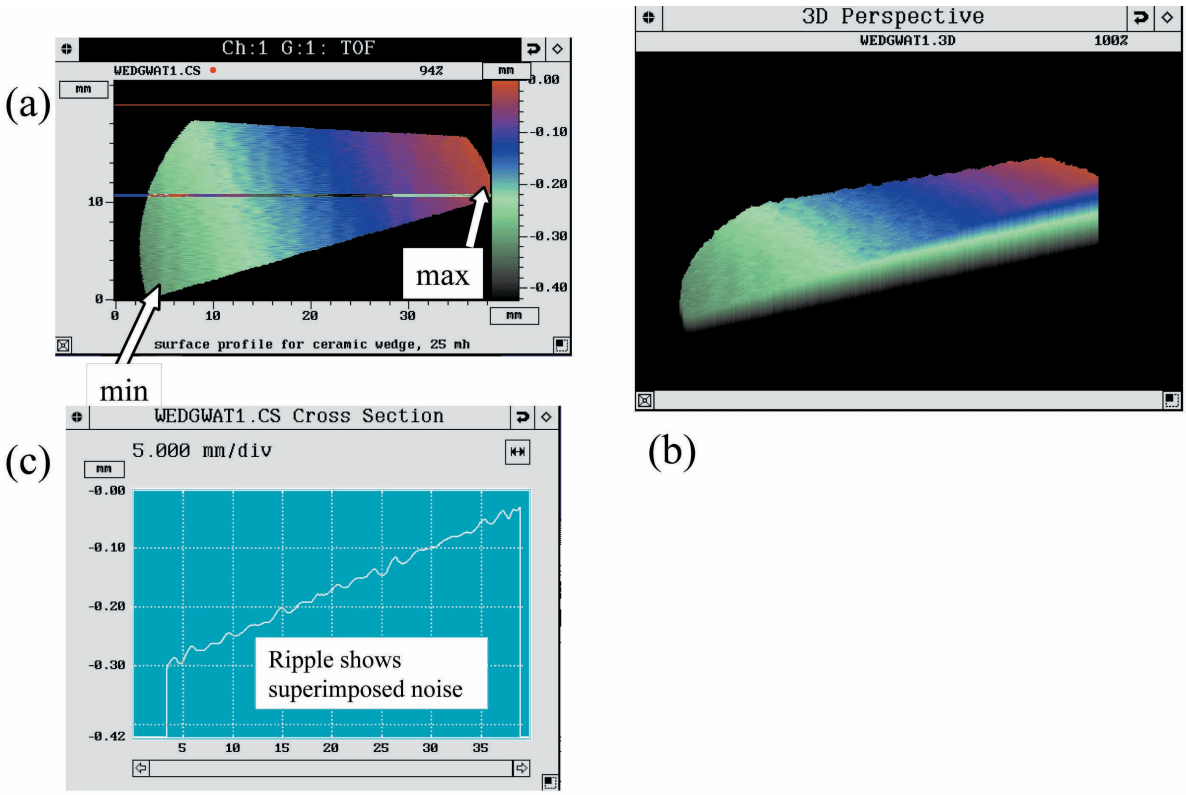

Figure 12. Ultrasonic surface profiles of ceramic wedge at 25 MHz. (a) Two-dimensional view (b) Three-dimensional view (c) Line profile across center of ceramic wedge as shown by line in (a). Profiles at 10 MHz were nearly identical.

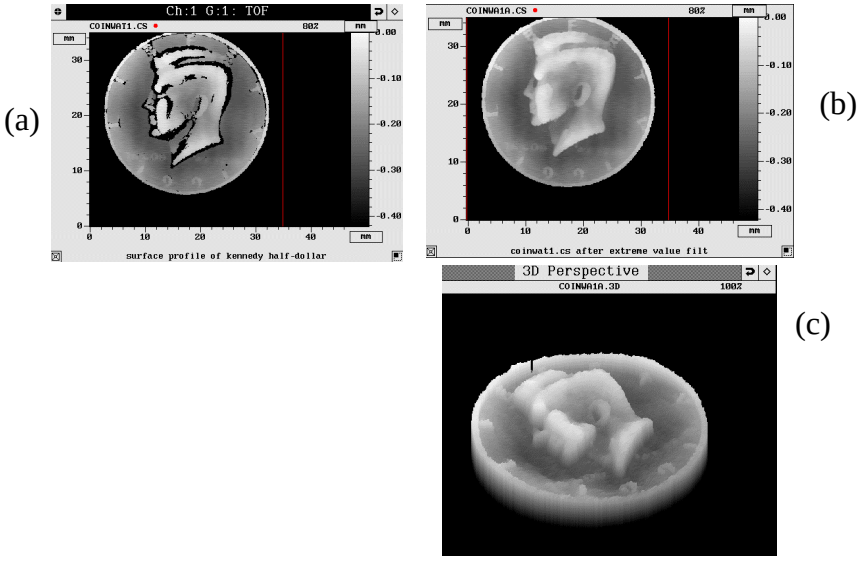

Figure 13. Ultrasonic surface profiles for Kennedy Half-dollar at 25 MHz. (a) Two-dimensional view. Black areas indicate where no ultrasound reflected back to the transducer (b) Two-dimensional view after replacement of black areas with nearest neighbors averaging-type software process (c) Three-dimensional view of (b).

(a)

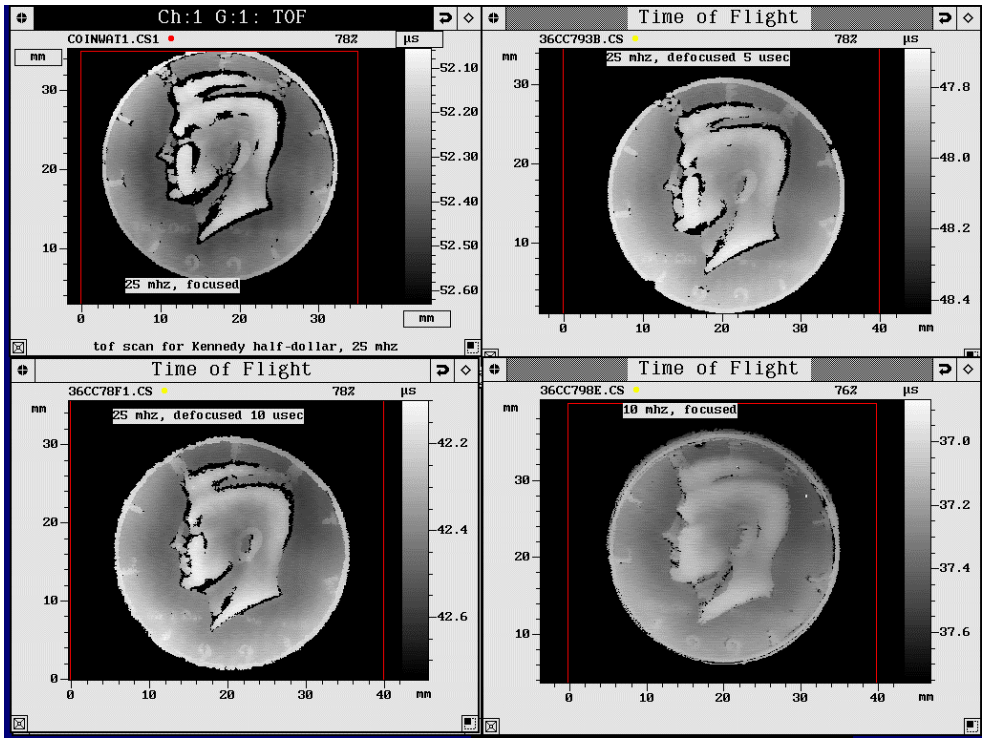

(b)

(c)

(d)

Figure 14. Ultrasonic surface profiles for Kennedy Half-dollar for 25 MHz focused, 25 MHz defocused, and 10 MHz focused. (a) 25 MHz focused. Black areas indicate where no ultrasound reflected back to the transducer (b) 25 MHz defocused by moving transducer closer to coin by 5 μsec (c) 25 MHz defocused by moving transducer closer to coin by 10 μsec (d) 10 MHz focused.

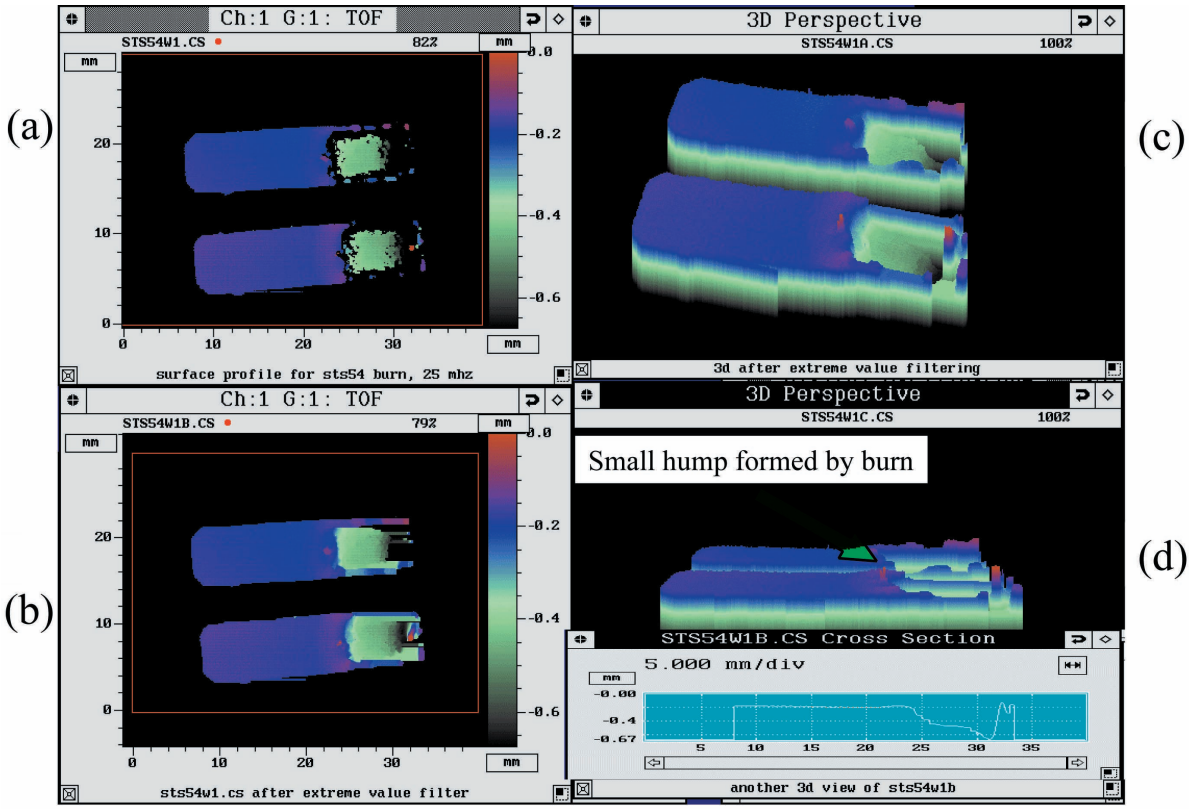

Figure 15. Ultrasonic surface profiles for Burned Space Experiment Samples at 25 Mhz (a) Two-dimensional view. Blackest areas indicate where no ultrasound reflected back to the transducer (b) Two-dimensional view after replacement of blackest areas with nearest neighbors averaging-type software process (c) Three-dimensional view (d) Another three-dimensional view also showing typical line profile.

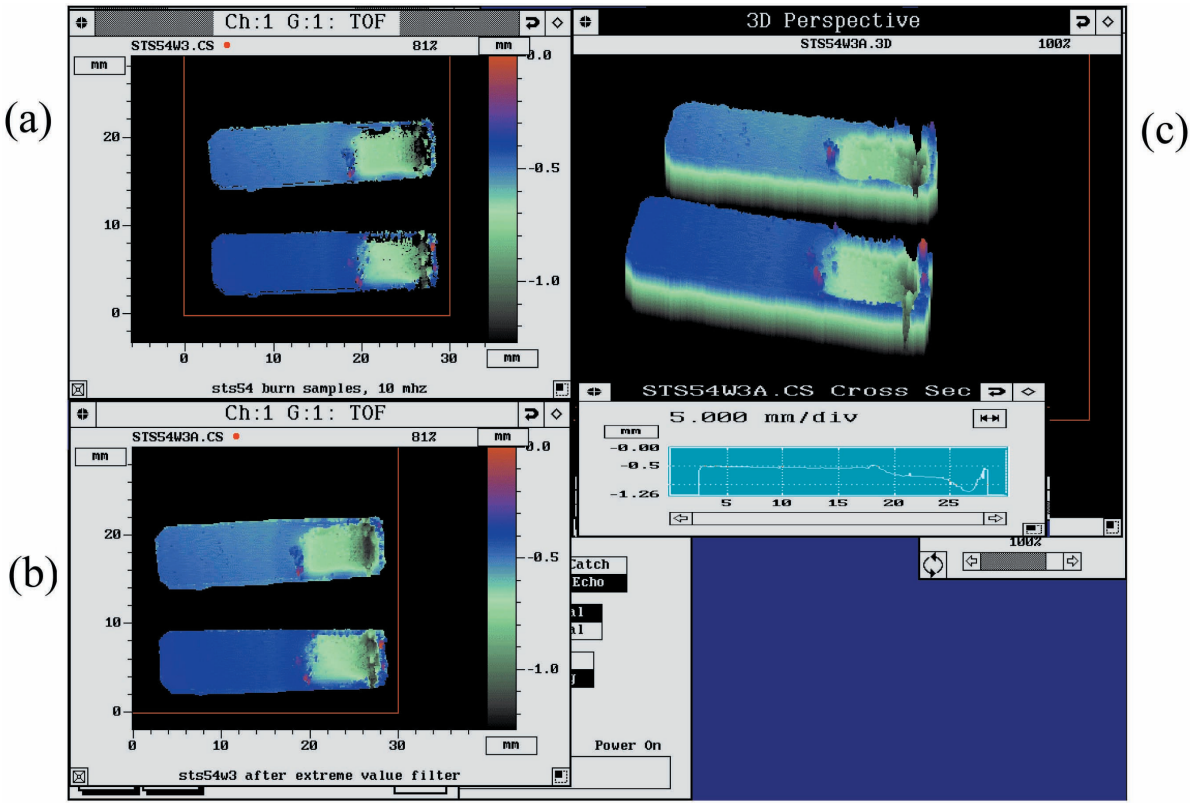

Figure 16. Ultrasonic surface profiles for Burned Space Experiment Samples at 10 MHz. (a) Two-dimensional view. Blackest areas indicate where no ultrasound reflected back to the transducer (b) Two-dimensional view after replacement of blackest areas with nearest neighbors averaging-type software process (c) Three-dimensional view with typical line profile.

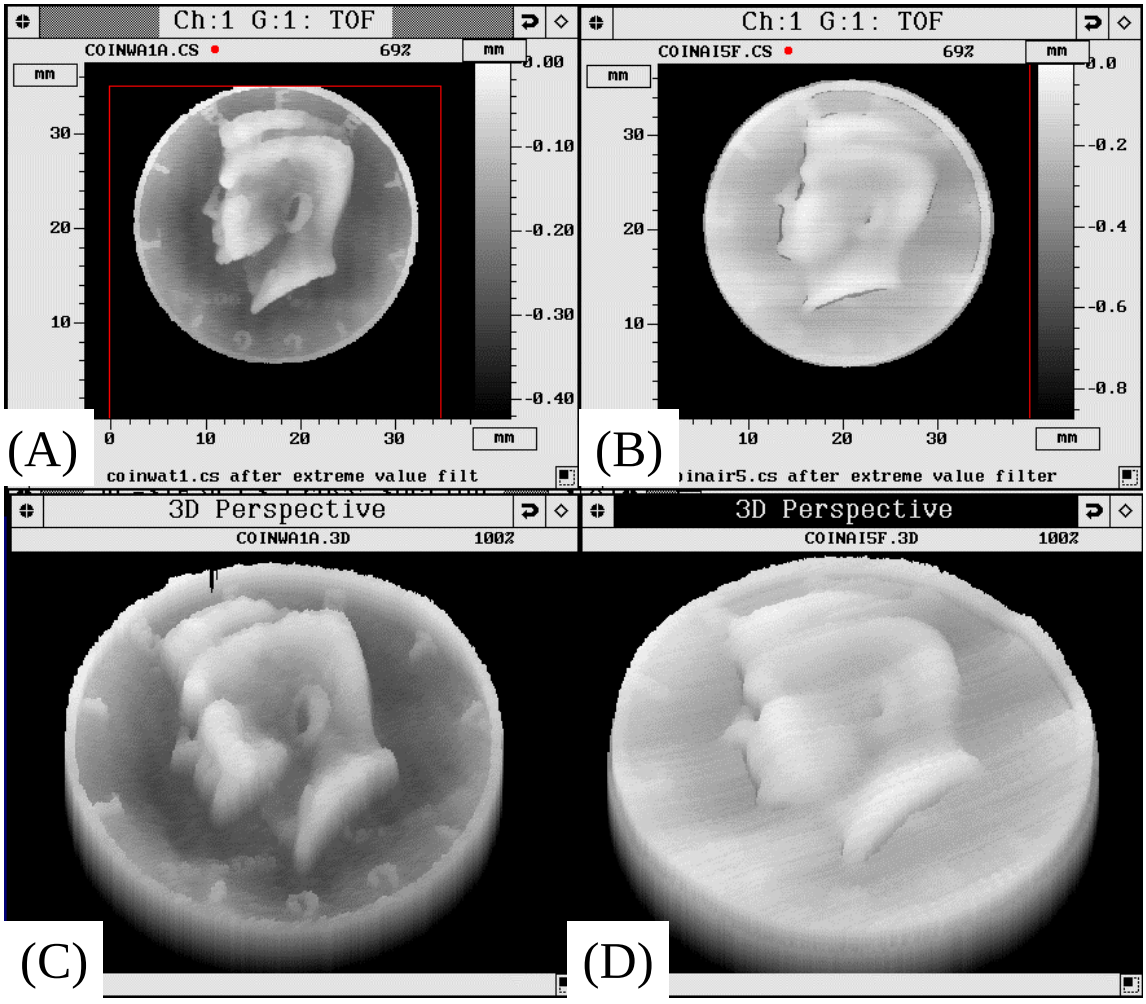

Figure 17. Water-coupled vs. Air-coupled Ultrasonic Surface Profiling. (a) 25 MHz water-coupled, two-dimensional view (b) 1 MHz air-coupled, two-dimensional view (c) 25 MHz water-coupled, three-dimensional view (d) 1 MHz air-coupled, three-dimensional view.

REPORT DOCUMENTATION PAGE

Form Approved
OMB No. 0704-0188

1. AGENCY USE ONLY (*Leave blank*)	2. REPORT DATE	3. REPORT TYPE AND DATES COVERED
	July 1999	Technical Memorandum

4. TITLE AND SUBTITLE

Using High Frequency Focused Water-Coupled Ultrasound for 3–D Surface Depression Profiling

5. FUNDING NUMBERS

WU–523–22–13–00

6. AUTHOR(S)

Don J. Roth, Mike F. Whalen, J. Lynne Hendricks, and James R. Bodis

7. PERFORMING ORGANIZATION NAME(S) AND ADDRESS(ES)

National Aeronautics and Space Administration
John H. Glenn Research Center at Lewis Field
Cleveland, Ohio 44135–3191

8. PERFORMING ORGANIZATION REPORT NUMBER

E–11715

9. SPONSORING/MONITORING AGENCY NAME(S) AND ADDRESS(ES)

National Aeronautics and Space Administration
Washington, DC 20546–0001

10. SPONSORING/MONITORING AGENCY REPORT NUMBER

NASA TM—1999-209268

11. SUPPLEMENTARY NOTES

Don J. Roth, NASA Glenn Research Center; Mike F. Whalen and J. Lynne Hendricks, Sonix, Inc., Springfield, Virginia 22152; and James R. Bodis, Cleveland State University, Cleveland, Ohio 44115. Funding for this work came from the NASA HITEMP and COMMTECH programs and from Sonix, Inc. Responsible person, Don J. Roth, organization code 5920, (216) 433–6017.

12a. DISTRIBUTION/AVAILABILITY STATEMENT

Unclassified - Unlimited
Subject Category: 38 Distribution: Nonstandard

This publication is available from the NASA Center for AeroSpace Information, (301) 621–0390.

12b. DISTRIBUTION CODE

13. ABSTRACT ***(Maximum 200 words)***

Surface topography is an important variable in the performance of many industrial components and is normally measured with diamond-tip profilometry over a small area or using optical scattering methods for larger area measurement. A prior study was performed demonstrating that focused *air-coupled* ultrasound at 1 MHz was capable of profiling surfaces with 25 μm depth resolution and 400 μm lateral resolution over a 1.4 mm depth range. In this article, the question of whether higher-frequency focused water-coupled ultrasound can improve on these specifications is addressed. 10 and 25 MHz focused ultrasonic transducers were employed in the water-coupled mode. Time-of-flight images of the sample surface were acquired and converted to depth / surface profile images using the simple relation (d = V*t/2) between distance (d), time-of-flight (t), and the velocity of sound in water (V). Results are compared for the two frequencies used and with those from the 1 MHz air-coupled configuration.

14. SUBJECT TERMS

Nondestructive evaluation; Surface profilometry; Ultrasonics

15. NUMBER OF PAGES

29

16. PRICE CODE

A03

17. SECURITY CLASSIFICATION OF REPORT	18. SECURITY CLASSIFICATION OF THIS PAGE	19. SECURITY CLASSIFICATION OF ABSTRACT	20. LIMITATION OF ABSTRACT
Unclassified	Unclassified	Unclassified	